由 5-溴间苯二甲酸和 2,2′-联吡啶构筑的两个铜(Ⅱ)配合物的合成、晶体结构及磁性质

黎 彧*,1　邹训重1　冯安生1　赵振宇*,2

(1 广东轻工职业技术学院,广东省特种建筑材料及其绿色制备工程技术研究中心/
佛山市特种功能性建筑材料及其绿色制备技术工程中心,广州　510300)
(2 深圳信息职业技术学院智能制造与装备学院,深圳　518172)

摘要：采用水热方法,在 120 ℃温度下选用 5-溴间苯二甲酸(H₂BIPA)和 2,2′-联吡啶(2,2′-bipy)与 CuCl₂·2H₂O 分别在 NaOH 与 H₂BIPA 的物质的量之比为 2:1 和 3:1 时反应,得到了 1 个具有零维单核铜结构的配合物[Cu(BIPA)(2,2′-bipy)(H₂O)₂]·H₂O (1)和 1 个一维链状配位聚合物[Cu₃(μ₃-BIPA)₂(μ-OH)₂(2,2′-bipy)₂]ₙ (2),并对其结构和磁性质进行了研究。结构分析结果表明 2 个配合物均属于单斜晶系,分别为 P2₁/c 和 P2₁/n 空间群。配合物 1 具有零维单核铜结构,而且这些单核铜单元通过 O−H⋯O 氢键作用进一步形成了二维层。而配合物 2 具有基于三核铜单元的一维链结构。这些一维链通过链间的 π-π 相互作用进一步形成了二维层。2 个配合物的结构差异是由反应中 NaOH 与 H₂BIPA 的物质的量之比不同造成的。研究表明,配合物 2 的三核铜单元中相邻铜离子间存在反铁磁相互作用。

关键词：铜配合物；氢键；5-溴间苯二甲酸；磁性
中图分类号：O614.121　文献标识码：A　文章编号：1001-4861(2020)02-0345-07
DOI：10.11862/CJIC.2020.002

Syntheses, Crystal Structures and Magnetic Properties of Two Copper(Ⅱ) Coordination Compounds Based on 5-Bromoisophthalic Acid and 2,2′-Bipyridine

LI Yu*,1　ZOU Xun-Zhong1　FENG An-Sheng1　ZHAO Zhen-Yu*,2

(1Guangdong Research Center for Special Building Materials and Its Green Preparation Technology/Foshan
Research Center for Special Functional Building Materials and Its Green Preparation
Technology, Guangdong Industry Polytechnic, Guangzhou 510300, China)
(2School of Intelligent Manufacturing and Equipment, Shenzhen Institute of
Information Technology, Shenzhen, Guangdong 518172, China)

Abstract: Zero-dimensional mononuclear copper(Ⅱ) coordination compound and 1D chain copper(Ⅱ) coordination polymer, namely [Cu(BIPA)(2,2′-bipy)(H₂O)₂]·H₂O (**1**) and [Cu₃(μ₃-BIPA)₂(μ-OH)₂(2,2′-bipy)₂]ₙ (**2**), were constructed hydrothermally using H₂BIPA (H₂BIPA =5-bromoisophthalic acid), 2,2′-bipy (2,2′-bipy =2,2′-bipyridine), and copper chloride at the n_{NaOH}:n_{H_2BIPA} (molar ratio) of 2:1 or 3:1, respectively. Single-crystal X-ray diffraction analyses reveal that both compounds crystallize in the monoclinic system, space groups P2₁/c or P2₁/n, respectively. Compound **1** discloses a discrete monomer structure, which is assembled to a 2D sheet through O−H

···O hydrogen bonds. Compound **2** has a chain structure based on Cu$_3$ unit. The chains are further extended into a 2D sheet by π-π stacking interactions. Structural differences between compounds **1** and **2** are attributed to the different molar ratio between NaOH and H$_2$BIPA. Magnetic studies for compound **2** demonstrate an antiferromagnetic coupling between the adjacent Cu(II) centers within Cu$_3$ unit. CCDC: 1922559, **1**; 1922560, **2**.

0 Introduction

In recent years, great interest has been focused on the design and hydrothermal syntheses of functional coordination polymers owing to their intriguing architectures and topologies, as well as potential applications in catalysis, magnetism, luminescence and gas absorption[1-10]. Up to now, a large numbers of coordination polymers have been obtained by hydrothermal methods, which are optimal for crystal growth[1,3-4,11-13]. The mechanism of the complicated reactions under hydrothermal methods remain unclear, which depends directly on the interplay of starting materials, pH value, template, and reaction temperature[14-18].

In this regard, the selection of organic ligands is one of the most important aspects. Among a wide variety of organic ligands, various types of aromatic polycarboxylic acids have been proved to be versatile and efficient candidates for constructing diverse coordination polymers due to their rich coordination chemistry, tunable degree of deprotonation, and ability to act as H-bond acceptors and donors[15-16,18-22].

On the basis of the above account, we selected 5-bromoisophthalic acid (H$_2$BIPA) and investigated the influence of the reaction conditions on the structures of coordination polymers under hydrothermal conditions.

Herein, we report the syntheses, crystal structures, and magnetic properties of two Cu(II) coordination compounds constructed from 5-bromoisophthalic acid ligand.

1 Experimental

1.1 Reagents and physical measurements

All chemicals and solvents were of AR grade and used without further purification. Carbon, hydrogen and nitrogen were determined using an Elementar Vario EL elemental analyzer. IR spectra were recorded using KBr pellets and a Bruker EQUINOX 55 spectrometer. Thermogravimetric analysis (TGA) data were collected on a LINSEIS STA PT1600 thermal analyzer with a heating rate of 10 ℃·min^{-1}. Magnetic susceptibility data were collected in a temperature range of 2~300 K with a Quantum Design SQUID Magnetometer MPMS XL-7 with a field of 0.1 T. A correction was made for the diamagnetic contribution prior to data analysis.

1.2 Synthesis of [Cu(BIPA)(2,2′-bipy)(H$_2$O)$_2$]· H$_2$O (1)

A mixture of CuCl$_2$·2H$_2$O (0.017 g, 0.10 mmol), H$_2$BIPA (0.024 g, 0.10 mmol), 2,2′-bipyridine (2,2′-bipy, 0.016 g, 0.1 mmol), NaOH (0.008 g, 0.20 mmol) and H$_2$O (8 mL) was stirred at room temperature for 15 min, and then sealed in a 25 mL Teflon-lined stainless steel vessel, and heated at 120 ℃ for 3 days, followed by cooling to room temperature at a rate of 10 ℃·h^{-1}. Blue block-shaped crystals of **1** were isolated manually, and washed with distilled water. Yield: 58% (based on H$_2$BIPA). Anal. Calcd. for C$_{18}$H$_{17}$BrCuN$_2$O$_7$ (%): C 41.83, H 3.32, N 5.42; Found (%): C 42.05, H 3.34, N 4.39. IR (KBr, cm^{-1}): 3 444w, 3 238m, 1 593s, 1 543s, 1 476w, 1 420m, 1 354s, 1 248w, 1 174w, 1 091w, 1 063w, 1 030w, 901w, 763m, 724m, 661w, 594w, 546w.

1.3 Synthesis of [Cu$_3$(μ_3-BIPA)$_2$(μ-OH)$_2$(2,2′-bipy)$_2$]$_n$ (2)

Synthesis of **2** was similar to **1** except using a different amount of NaOH (0.012 g, 0.30 mmol). Blue block-shaped crystals of **2** were isolated manually, and washed with distilled water. Yield: 38 % (based on H$_2$BIPA). Anal. Calcd. for C$_{36}$H$_{24}$Br$_2$Cu$_3$N$_4$O$_{10}$(%): C 42.26, H 2.36, N 5.48; Found(%): C 42.03, H 2.35, N 5.51. IR (KBr, cm^{-1}): 3 423w, 3 055w, 1 627m, 1 604s,

1 576m, 1 555m, 1 494w, 1 427w, 1 370m, 1 326s, 1 248 w, 1 158w, 1 119w, 1 086w, 1 024w, 886w, 767m, 728m, 657w, 634w, 546w. The compounds are insoluble in water and common organic solvents, such as methanol, ethanol, acetone and DMF.

1.4 Structure determinations

Two single crystals with dimensions of 0.26 mm× 0.23 mm×0.22 mm (**1**) and 0.25 mm×0.18 mm×0.16 mm (**2**) were collected at 293(2) K on a Bruker SMART APEX Ⅱ CCD diffractometer with Mo $K\alpha$ radiation (λ =0.071 073 nm). The structures were solved by direct methods and refined by full matrix least-square on F^2 using the SHELXTL-2014 program[23]. All non-hydrogen atoms were refined anisotropically. All the hydrogen atoms were positioned geometrically and refined using a riding model. A summary of the crystallography data and structure refinements for **1** and **2** is given in Table 1. The selected bond lengths and angles for compounds **1** and **2** are listed in Table 2. Hydrogen bond parameters of compounds **1** and **2** are given in Table 3.

CCDC: 1922559, **1**; 1922560, **2**.

Table 1　Crystal data for compounds 1 and 2

Compound	1	2
Chemical formula	$C_{18}H_{17}BrCuN_2O_7$	$C_{36}H_{24}Br_2Cu_3N_4O_{10}$
Molecular weight	516.78	1 023.03
Crystal system	Monoclinic	Monoclinic
Space group	$P2_1/c$	$P2_1/n$
a / nm	2.062 7(2)	0.985 21(4)
b / nm	0.783 37(5)	1.741 02(7)
c / nm	2.374 67(17)	1.030 43(7)
β / (°)	91.907(7)	99.378(5)
V / nm³	3.835 0(5)	1.743 84(16)
Z	8	2
$F(000)$	2 072	1 010
θ range for data collection / (°)	3.286~25.050	3.538~25.044
Limiting indices	$-24 \leqslant h \leqslant 24, -9 \leqslant k \leqslant 8, -28 \leqslant l \leqslant 22$	$-9 \leqslant h \leqslant 11, -18 \leqslant k \leqslant 20, -11 \leqslant l \leqslant 12$
Reflection collected, unique (R_{int})	13 849, 6 782 (0.082 2)	5 731, 3 084 (0.033 4)
D_c / (g·cm⁻³)	1.790	1.948
μ / mm⁻¹	3.268	4.172
Data, restraint, parameter	6 782, 0, 523	3 084, 0, 254
Goodness-of-fit on F^2	1.000	1.048
Final R indices [$I \geqslant 2\sigma(I)$] R_1, wR_2	0.060 8, 0.084 7	0.041 7, 0.093 7
R indices (all data) R_1, wR_2	0.116 4, 0.146 7	0.061 8, 0.107 2
Largest diff. peak and hole / (e·nm⁻³)	915 and −534	1 234 and −708

Table 2　Selected bond lengths (nm) and bond angles (°) for compounds 1 and 2

1					
Cu(1)-O(2)	0.197 1(5)	Cu(1)-O(9)	0.197 1(5)	Cu(1)-O(10)	0.223 6(5)
Cu(1)-N(1)	0.200 2(7)	Cu(1)-N(2)	0.200 3(6)	Cu(2)-O(5)	0.197 2(5)
Cu(2)-O(11)	0.224 2(4)	Cu(2)-O(12)	0.195 7(5)	Cu(2)-N(3)	0.202 6(6)
Cu(2)-N(4)	0.200 7(6)				
O(9)-Cu(1)-O(2)	93.6(2)	O(9)-Cu(1)-N(1)	93.3(2)	O(2)-Cu(1)-N(1)	168.4(3)
O(9)-Cu(1)-N(2)	164.4(2)	O(2)-Cu(1)-N(2)	90.6(3)	N(2)-Cu(1)-N(1)	80.3(3)
O(9)-Cu(1)-O(10)	90.96(19)	O(2)-Cu(1)-O(10)	96.7(2)	N(1)-Cu(1)-O(10)	92.5(2)

Continued Table 1

N(2)-Cu(1)-O(10)	103.5(2)	O(5)-Cu(2)-O(12)	94.0(2)	O(12)-Cu(2)-N(4)	165.1(2)
O(5)-Cu(2)-N(4)	90.0(2)	O(12)-Cu(2)-N(3)	93.8(2)	O(5)-Cu(2)-N(3)	168.0(2)
N(4)-Cu(2)-N(3)	80.3(3)	O(12)-Cu(2)-O(11)	91.90(19)	O(11)-Cu(2)-O(5)	98.40(19)
N(4)-Cu(2)-O(11)	101.8(2)	N(3)-Cu(2)-O(11)	90.4(2)		
		2			
Cu(1)-O(1)	0.193 0(3)	Cu(1)-O(3)A	0.264 9(4)	Cu(1)-O(5)	0.190 2(4)
Cu(1)-N(1)	0.200 1(4)	Cu(1)-N(2)	0.202 2(4)	Cu(2)-O(4)A	0.195 2(3)
Cu(2)-O(4)B	0.195 2(3)	Cu(2)-O(5)	0.192 2(4)	Cu(2)-O(5)C	0.192 2(4)
O(5)-Cu(1)-O(1)	97.96(15)	O(5)-Cu(1)-N(1)	92.83(16)	O(1)-Cu(1)-N(1)	164.80(16)
O(5)-Cu(1)-N(2)	169.39(16)	O(1)-Cu(1)-N(2)	90.64(14)	N(1)-Cu(1)-N(2)	79.96(15)
O(1)-Cu(1)-O(3)A	100.94(15)	O(5)-Cu(1)-O(3)A	79.77(14)	N(1)-Cu(1)-O(3A)	91.46(15)
N(2)-Cu(1)-O(3A)	92.57(15)	O(5)-Cu(2)-O(4)A	91.76(14)	O(5)-Cu(2)-O(4)B	88.24(14)

Symmetry codes: A: $x+1$, y, z; B: $-x+1$, $-y$, $-z+1$; C: $-x+2$, $-y$, $-z+1$ for **2**.

Table 3　Hydrogen bond parameters of compounds 1 and 2

Compound	D−H⋯A	d(D-H) / nm	d(H⋯A) / nm	d(D⋯A) / nm	∠DHA / (°)
1	O(9)−H(1W)⋯O(1)	0.087 6	0.178 1	0.256 0	147.0
	O(9)−H(2W)⋯O(7)A	0.087 7	0.181 1	0.266 9	165.3
	O(10)−H(3W)⋯O(8)A	0.086 8	0.193 7	0.279 8	171.2
	O(10)−H(4W)⋯O(7)B	0.085 0	0.183 1	0.268 1	179.1
	O(11)−H(5W)⋯O(4)C	0.086 1	0.197 0	0.269 3	140.9
	O(11)−H(6W)⋯O(3)D	0.085 0	0.195 9	0.280 9	179.5
	O(12)−H(7W)⋯O(4)D	0.085 0	0.185 7	0.270 7	179.1
	O(12)−H(8W)⋯O(6)	0.087 4	0.178 5	0.255 6	145.8
	O(13)−H(9W)⋯O(8)A	0.085 0	0.204 4	0.289 4	179.1
	O(14)−H(11W)⋯O(3)E	0.085 0	0.196 8	0.281 6	175.3
2	O(5)−H(1)⋯O(2)	0.076 0	0.215 1	0.281 6	146.5

Symmetry codes: A: $-x$, $y+1/2$, $-z+1/2$; B: x, $y+1$, z; C: x, $y-1$, z; D: $-x+1$, $y-1/2$, $-z+1/2$; E: $-x+1$, $y+1/2$, $-z+1/2$ for **1**.
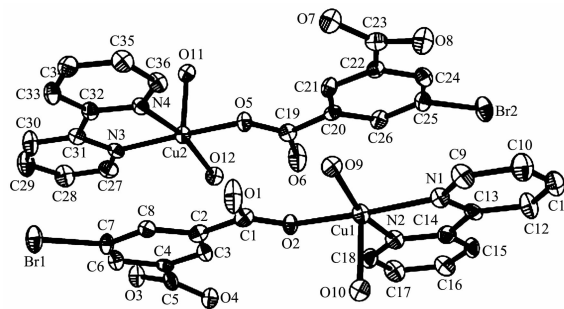
2　Results and discussion

2.1　Description of the structure

2.1.1　[Cu(BIPA)(2,2′-bipy)(H₂O)₂]·H₂O (**1**)

Single-crystal X-ray diffraction analysis reveals that compound **1** crystallizes in the monoclinic space group $P2_1/c$. Its asymmetric unit contains two mononuclear copper(II) units and two lattice water molecules (Fig.1). In each [Cu(BIPA)(2,2′-bipy)(H₂O)₂] unit, the Cu(II) ions are five-coordinated and form a distorted square-pyramidal {CuN₂O₃} geometry with the τ parameters of 0.066 7 or 0.048 3 (τ=0 or 1 for a regular square-pyramidal or trigonal-bipyramidal geometry, respectively)[24]. It is taken by a carboxylate O atom of BIPA²⁻,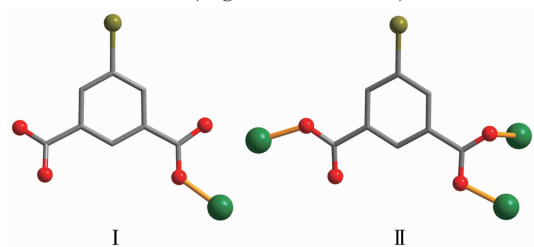 two H₂O ligands, and two N donors from the 2,2′-bipy ligand. The Cu-O bonds (0.195 7(5) ~0.224 2(4) nm) and the Cu-N distances (0.200 2(7)~ 0.202 6(6) nm) agree with literature data[3,22,25]. In **1**, the BIPA²⁻ moiety acts as a terminal ligand (mode Ⅰ,
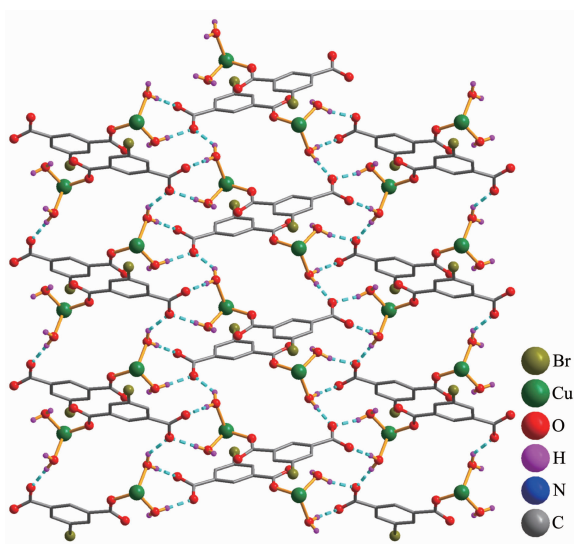

H atoms and lattice water molecules were omitted for clarity

Fig.1　Drawing of asymmetric unit of compound **1** with 30% probability thermal ellipsoids

Scheme 1). Discrete mononuclear copper(Ⅱ) units are assembled, via the O−H···O hydrogen bonds, into a 2D H-bonded sheet (Fig.2 and Table 3).

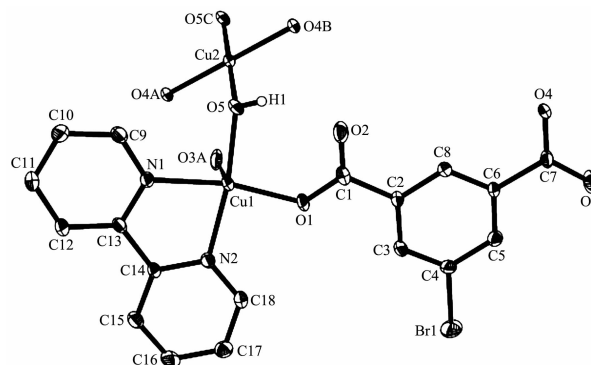Scheme 1　Coordination modes of BIPA^{2-} ligands in compounds **1** and **2**

Dashed lines present the H-bonds

Fig.2　Perspective of 2D sheet in **1**

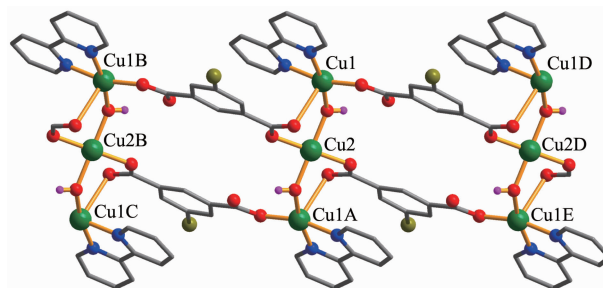### 2.1.2　[Cu$_3$(μ_3-BIPA)$_2$(μ-OH)$_2$(2,2'-bipy)$_2$]$_n$ (**2**)

The asymmetric unit of **2** consists of two Cu(Ⅱ) ions (Cu1 with full occupancy and Cu2 with half occupancy), one μ_3-BIPA^{2-} block, one 2,2'-bipy ligand, and μ-OH$^-$ linker. As shown in Fig.3, five-coordinated Cu1 atom reveals a distorted square-pyramidal {CuN$_2$O$_3$} geometry with the τ parameters of 0.076 5, filled by two carboxylate O atoms from two individual μ_3-BIPA^{2-} blocks, one O atom from the μ-OH$^-$ linker, and a pair of N atoms from 2,2'-bipy ligand. The four-coordinated Cu2 atom shows a distorted {CuN$_2$O$_2$} square-planar geometry, which is taken by two carboxylate O atoms from two different BIPA^{2-} blocks and two O atoms from two individual μ-OH$^-$ linkers. The Cu-O lengths range from 0.190 2(4) to 0.264 9(4) nm, whereas the Cu-N lengths vary from 0.200 1(4) to

0.202 2(4) nm; these bonding parameters are comparable to those observed in other Cu(Ⅱ) compounds[3,22,25]. In **2**, the BIPA^{2-} block acts as a μ_3-linker, and its COO$^-$ groups are monodentate or bidentate (mode Ⅱ, Scheme 1). The three adjacent Cu(Ⅱ) ions are bridged by means of two carboxylate groups from two different BIPA^{2-} blocks and two μ-OH$^-$ linkers, giving rise to a trinuclear copper(Ⅱ) subunit (Fig.4). In this Cu$_3$ subunit, the Cu1···Cu2 distance is 0.344 1(4) nm. The neighboring Cu$_3$ subunits are multiply interlinked by BIPA^{2-} blocks into a 1D chain (Fig.4), having the shortest distance of 0.985 2 nm between the adjacent trinuclear copper(Ⅱ) subunits. The intrachain (N1/C9-C13 and C2A-C7A, Cg···Cg 0.374 6(2) nm, Symmetry code: A: x+1, y, z) and interchain (N2/C14-C18 and C2B-C7B, Cg···Cg 0.352 1(2) nm, Symmetry code: B: x+1/2, $-y$+1/2, z+1/2) π-π stacking interactions between adjacent pyridyl planes of the 2,2'-bipy ligands and the benzene planes of BIPA^{2-} blocks are observed (Fig.5).

H atoms and lattice water molecules were omitted for clarity except H of OH$^-$ group; Symmetry codes: A: x+1, y, z; B: $-x$+1, $-y$, $-z$+1; C: $-x$+2, $-y$, $-z$+1
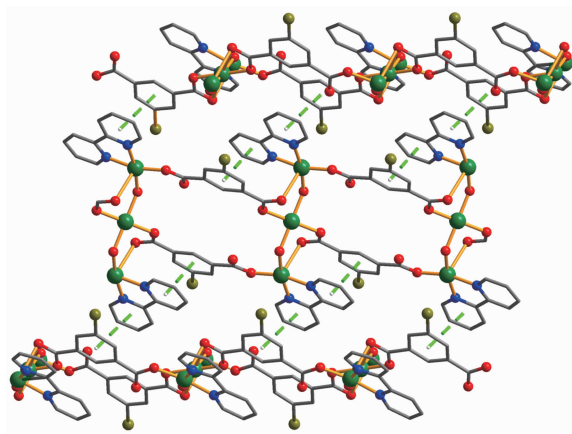
Fig.3　Drawing of asymmetric unit of compound **2** with 30% probability thermal ellipsoids

Symmetry codes: A: $-x$+2, $-y$, $-z$; B: x−1, y, z; C: $-x$+1, $-y$, $-z$+1; D: x+1, y, z; E: $-x$+3, $-y$, $-z$+1

Fig.4　One-dimensional chain viewed along c axis in **2**

The chains are further extended into a 2D sheet by π-π stacking interactions (Fig.5).

Dashed lines present the π-π stacking interactions

Fig.5　Two-dimensional sheet viewed along c axis in **2**

2.2　TGA analysis

To determine the thermal stability of compounds **1** and **2**, their thermal behaviors were investigated under nitrogen atmosphere by thermogravimetric analysis (TGA). As shown in Fig.6, compound **1** lost its one lattice and two coordinated water molecules in a range of 43~122 ℃ (Obsd. 10.1%; Calcd. 10.4%), followed by the decomposition at 234 ℃. The TGA curve of **2** reveals that compound **2** was stable up to 241 ℃, then was decomposed upon further heating.
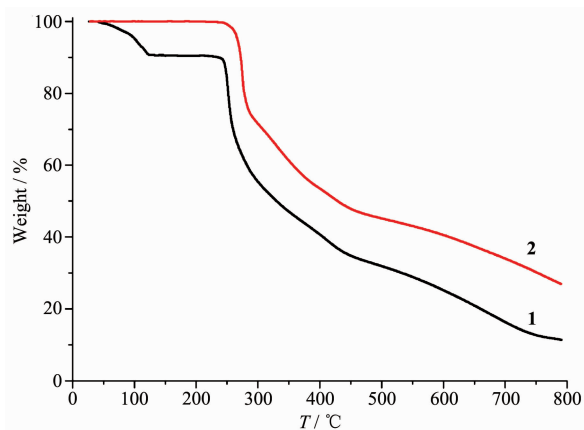

Fig.6　TGA curves of compounds **1** and **2**
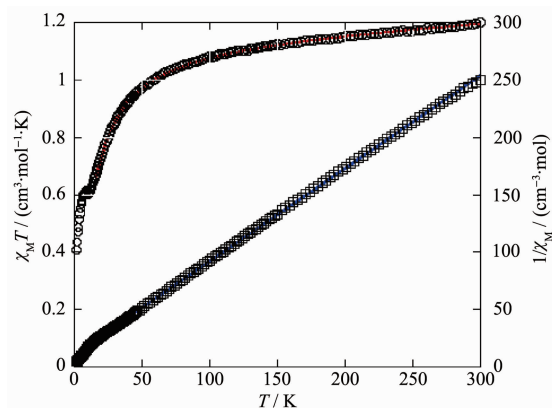
2.3　Magnetic properties

Variable-temperature magnetic susceptibility studies were carried out on powder sample of **2** in a temperature range of 2~300 K (Fig.7). The $\chi_M T$ value at 300 K was 1.20 cm³·mol⁻¹·K, which is slightly higher than the value (1.125 cm³·mol⁻¹·K) expected for three magnetically isolated Cu(Ⅱ) centers (S_{Cu}=1/2, g =2.0). Upon cooling, the $\chi_M T$ value decreased to reach a plateau around 11 ~7 K with $\chi_M T$ value of 0.608~0.598 cm³·mol⁻¹·K, and finally went down to 0.406 cm³·mol⁻¹·K at 2 K. The plateau corresponds to the ground state (S=1/2). In the 15~300 K interval, the χ_M^{-1} vs T plot for **2** obeys the Curie-Weiss law with a Weiss contant θ of −25.3 K and a Curie constant C of 1.26 cm³·mol⁻¹·K. Although the separation between the adjacent Cu₃ subunits are somewhat longer, the magnetic exchange coupling mediated by spin-polarization mechanism through the intrachain and interchain π-π stacking interactions[26-28]. Because the magnetic exchange coupling through π-π stacking interactions is assumed to be weaker than the intratrinuclear interactions, the negative value of θ and the decrease in $\chi_M T$ should be attributed to the overall antiferromagnetic coupling between the Cu(Ⅱ) ions within the Cu₃ subunit.

The spin Hamiltonian appropriate for describing the magnetic properties of an isolated linear trinuclear system is given in Eq.(1):

$$H_{exp}=-2J(S_1S_2+S_2S_3)-2J'(S_1S_3) \tag{1}$$

Where J denotes the exchange parameter between the central and terminal copper(Ⅱ) ions, and J' is assumed to be zero since the distance between the two terminal Cu(Ⅱ) ions is so large (0.688 3 nm). The magnetic properties were analyzed using Eq.(2), derived from Eq.(1) for a linear trinuclear model with S=1/2[29]:

Red curve represents the best fit to the equations in the text, and the blue line shows the Curie-Weiss fitting

Fig.7　Temperature dependence of $\chi_M T$ (○) and $1/\chi_M$ (□) vs T for compound **2**

$$\chi_{\mathrm{M}} = \frac{Ng^2\beta^2}{3k(T-\theta)}\frac{(1+\mathrm{e}^{-\frac{2J}{kT}}+10\mathrm{e}^{-\frac{2J}{kT}})}{(1+\mathrm{e}^{-\frac{2J}{kT}}+2\mathrm{e}^{-\frac{2J}{kT}})}N_\alpha \qquad (2)$$

Where θ is a Weiss-like correction for intermolecular interactions, and N_α is temperature independent paramagnetism. Using this method, the susceptibilities for **2** above 15.0 K were simulated, and the best-fit parameters for **2** were obtained: $J=-35.6$ cm^{-1}, $g=2.11$, $\theta=-0.47$ K, $N_\alpha=3.60\times10^{-4}$ cm$^3\cdot$mol^{-1} and $R=5.2\times10^{-5}$, where $R=\sum(T_{\mathrm{obs}}-T_{\mathrm{calc}})^2/\sum(T_{\mathrm{obs}})^2$. The J value of -35.6 cm^{-1} indicates that the coupling between the adjacent Cu(Ⅱ) centers is antiferromagnetic. According to the structure of compound **2**, there are two sets of magnetic exchange pathways within the trinuclear copper(Ⅱ) cores, namely, via the μ-OH$^-$ groups and μ-carboxylates bridges (Fig.4), which can be responsible for the observed antiferromagnetic exchange.

3　Conclusions

In summary, we have synthesized two Cu(Ⅱ) coordination compounds whose structures depend on the molar ratio between NaOH and H$_2$BIPA. This work demonstrates that the molar ratio between NaOH and carboxylic acid ligand has a significant effect on the structures of Cu(Ⅱ) coordination compounds.

References:

[1] Lu W G, Su C Y, Lu T B, et al. *J. Am. Chem. Soc.*, **2006**, **128**:34-35

[2] Zhen X D, Lu T B. *CrystEngComm*, **2010**,**12**:324-336

[3] Gu J Z, Wen M, Cai Y, et al. *Inorg. Chem.*, **2019**,**58**:2403-2412

[4] Gu J Z, Wen M, Cai Y, et al. *Inorg. Chem.*, **2019**,**58**:5875-5885

[5] Jain P, Ramachandran V, Clark R J, et al. *J. Am. Chem. Soc.*, **2009**,**131**:13625-13627

[6] Minguez E G, Coronado E. *Chem. Soc. Rev.*, **2018**,**47**:533-557

[7] Cui Y J, Yue Y F, Qian G D, et al. *Chem. Rev.*, **2012**,**112**:1126-1162

[8] Zhao J, Wang Y N, Dong W W, et al. *Inorg. Chem.*, **2016**,**55**:3265-3271

[9] Zhu J, Usov P M, Xu W Q, et al. *J. Am. Chem. Soc.*, **2018**,**140**:993-1003

[10]Fu H R, Zhao Y, Zhou Z, et al. *Dalton Trans.*, **2018**,**47**:3725-3732

[11]Gu J Z, Liang X X, Cai Y, et al. *Dalton Trans.*, **2017**,**46**:10908-10925

[12]Gu J Z, Liang X X, Cui Y H, et al. *CrystEngComm*, **2017**,**19**:117-128

[13]Ma D Y, Qin L, Lei J M, et al. *CrystEngComm*, **2016**,**18**:1363-1375

[14]Mao N N, Hu P, Yu F, et al. *CrystEngComm*, **2017**,**19**:4586-4594

[15]Gu J Z, Cai Y, Qian Z Y, et al. *Dalton Trans.*, **2018**,**47**:7431-7444

[16]Gu J Z, Gao Z Q, Tang Y. *Cryst. Growth Des.*, **2012**,**12**:3312-3323

[17]ZOU Xun-Zhong(邹训重), WU Jiang(吴疆), GU Jin-Zhong(顾金忠), et al. *Chinese J. Inorg. Chem.*(无机化学学报), **2019**,**35**(9):1705-1711

[18]Gu J Z, Cui Y H, Liang X X, et al. *Cryst. Growth Des.*, **2016**,**16**:4658-4670

[19]Peng Y W, Wu R J, Liu M, et al. *Cryst. Growth Des.*, **2019**,**19**:1322-1328

[20]GU Wen-Jun(顾文君), GU Jin-Zhong(顾金忠). *Chinese J. Inorg. Chem.*(无机化学学报), **2017**,**33**(2):227-236

[21]ZHAO Su-Qin(赵素琴), GU Jin-Zhong(顾金忠). *Chinese J. Inorg. Chem.*(无机化学学报), **2016**,**32**(9):1611-1618

[22]Gu J Z, Liang X X, Cai Y, et al. *Dalton Trans.*, **2017**,**46**:10908-10925

[23]Spek A L. *Acta Crystallogr. Sect. C: Struct. Chem.*, **2015**, **C71**:9-18

[24]Addison A W, Rao T N, Reedijk J, et al. *J. Chem. Soc. Dalton Trans.*, **1984**,**7**:1349-1356

[25]Dey S K, Shit S, Mitra S, et al. *Inorg. Chim. Acta*, **2007**,**360**:1915-1920

[26]Spielberg E T, Fittipaldi M, Geibig D, et al. *Inorg. Chim. Acta*, **2010**,**363**:4269-4276

[27]Fernandes T S, Vilela R S, Valdo A K, et al. *Inorg. Chem.*, **2016**,**55**:2390-2401

[28]Glaser T, Heidemeier M, Strautmann J B H, et al. *Chem. Eur. J.*, **2007**,**13**:9191-9206

[29]Bonner J C, Fisher M E. *Phys. Rev. A*, **1964**,**135**:640-658